Structural stability and decomposition of Mg(BH$_4$)$_2$ isomorphs—an *ab initio* free energy study

FAST TRACK COMMUNICATION

Structural stability and decomposition of Mg(BH₄)₂ isomorphs—an *ab initio* free energy study

J Voss[1,2], J S Hummelshøj[1,2], Z Łodziana[3] and T Vegge[1]

[1] Materials Research Division, Risø National Laboratory for Sustainable Energy, Technical University of Denmark, Roskilde, Denmark
[2] Center for Atomic-scale Materials Design, Department of Physics, Technical University of Denmark, Kongens Lyngby, Denmark
[3] Department of Mobility, Environment, and Energy, EMPA Materials Sciences and Technology, Dübendorf, Switzerland

E-mail: tejs.vegge@risoe.dk

Abstract

We present the first comprehensive comparison between free energies, based on a phonon dispersion calculation within density functional theory, of theoretically predicted structures and the experimentally proposed α ($P6_1$) and β ($Fddd$) phases of the promising hydrogen storage material $Mg(BH_4)_2$.

The recently proposed low-density $I\bar{4}m2$ ground state is found to be thermodynamically unstable, with soft acoustic phonon modes at the Brillouin zone boundary. We show that such acoustic instabilities can be detected by a macroscopic distortion of the unit cell. Following the atomic displacements of the unstable modes, we have obtained a new $F222$ structure, which has a lower energy than all previously experimentally and theoretically proposed phases of $Mg(BH_4)_2$ and is free of imaginary eigenmodes. A new meta-stable high-density $I4_1/amd$ structure is also derived from the $I\bar{4}m2$ phase.

Temperatures for the decomposition are found to be in the range of 400–470 K and largely independent of the structural complexity, as long as the primary cation coordination polyhedra are properly represented. This opens a possibility of using simple model structures for screening and prediction of finite temperature stability and decomposition temperatures of novel borohydride systems.

S Supplementary data are available from stacks.iop.org/JPhysCM/21/012203

1. Introduction

The search for novel hydrogen storage materials which combine high hydrogen content with the potential for reversible storage under near ambient conditions has directed the focus from alanates to borohydride systems. The binary alkali borohydrides, e.g. $LiBH_4$ [1, 2], are found to be too thermodynamically stable, whereas the divalent $Ca(BH_4)_2$ and in particular $Mg(BH_4)_2$ have extracted interest, since empirical [3] and density functional theory (DFT) calculations on model structures [4] have indicated highly favorable thermodynamic properties.

Although originally synthesized in 1950 [5], a specific crystal structure was not proposed for $Mg(BH_4)_2$ until 2007, when Černý *et al* [6] and Her *et al* [7], independently, proposed a hexagonal 'low-temperature' (α) $P6_1$ phase consisting of 330 atoms in the unit cell and a density of $\rho = 0.78$ g cm^{-3}. Her *et al* [7] furthermore proposed an anti-phase boundary modification of an orthorhombic $Fddd$ super structure (704 atoms) as a 'high-temperature' (β) phase ($\rho = 0.76$ g cm^{-3}), and observed at least one additional modification. Chłopek *et al* [8] have presented XRD and DSC data, which indicates that even the $P6_1$ (α) phase could be meta-stable. Neither

of these structures can, however, account for the tetragonal, high-density ($\rho = 0.99$ g cm^{-3}) phase originally obtained by Konoplev and Bukulina in 1971 [9], using a different synthesis procedure.

Prior to the characterization of the α-phase, a number of simpler structures had been proposed on the basis of density functional theory (DFT) calculations: a hexagonal structure in space group $P\bar{3}m1$ [4] and a orthogonal structure in space group $Pmc2_1$ [10]; recently, the ground state energies of the α and β phases were calculated independently by Ozolins *et al* [11] and Dai *et al* [12]. Van Setten *et al* [13] later estimated free energies from the Γ-point frequencies, excluding unstable modes with larger wavevectors, that lead to larger structures with lower energies.

The phase stability can only be determined from the free energy, and we present the first direct comparison of free energies based on the calculation of the phonon dispersion of the most stable theoretically predicted structures and the experimentally proposed α and β super-structures, yielding surprisingly small differences between ground state energies and free energies of these structures.

Based on a vibrational analysis of the recently proposed low-density $I\bar{4}m2$ phase [11], which indicates thermodynamic instability of this phase, we obtain a new $F222$ structure of Mg(BH$_4$)$_2$. We find the $F222$ phase to have a lower free energy than any other proposed experimental or theoretical structure. We also identify the existence of a new meta-stable high-density ($\rho = 1.01$ g cm^{-3}) tetragonal $I4_1/amd$ structure without instabilities, which may account for the experimentally observed and uncharacterized tetragonal high-density structure ($\rho = 0.99$ g cm^{-3}) [9]. This phase can be interpreted as a folded form of the low-density $I\bar{4}m2$ structure ($\rho = 0.56$ g cm^{-3}).

We believe that the specific conditions of the current chemical synthesis procedure [8] combined with kinetically limited phase transitions between the large super-structures could account for the lack of (recent) experimental observations of $F222$ or $I4_1/amd$, and we anticipate future experimental verification of a highly complex phase diagram, similar to that of Ca(BH$_4$)$_2$ [14], e.g., by use of high pressure experiments.

The calculations also show that the thermodynamic properties of even highly complex borohydride super-structures can be well estimated by DFT using even simple model structures, if the primary coordination polyhedra are correctly accounted for. A purely thermodynamic estimate, i.e. not considering the inherently slow kinetics of borohydride systems [8], of the decomposition temperature yields values of 400–470 K for the idealized decomposition, Mg(BH$_4$)$_2$ → MgH$_2$ + 2B + 3H$_2$, for the complex and the simple unit cell structures.

These findings enable faster screening studies of thermodynamic stability and decomposition temperatures for, e.g., ternary and quaternary borohydride systems; not only in terms of reduced computational effort due to smaller system sizes, but also with the advantage that the exact space group need not be known *a priori*.

2. Computational details

Total energies and gradients were calculated within density functional theory [15] (DFT) using the Vienna *ab initio* Simulation Package (VASP) [16]. The Kohn–Sham wavefunctions [17] were expanded in plane-wave basis sets with energy cut-offs of up to 500 eV. Brillouin zone sampling was performed on meshes with a k-point spacing of $\leqslant 0.03$ Å^{-1} (for the larger $P6_1$ and $Fddd$ structures, the spacing was $\leqslant 0.06$ Å^{-1}). The Perdew-Wang-91 exchange–correlation functional [18, 19] was used in combination with the projector-augmented wave method [20], using parametrizations due to Kresse and Joubert [21].

Phonon dispersions and phonon densities of states were calculated by the direct method in the harmonic approximation with the software package Phonon [22], using the Hellmann–Feynman forces from minimal sets of atomic displacements. To resolve inter-atomic couplings, super-cells containing no less than eight formula units of Mg(BH$_4$)$_2$ were used.

Due to the large system sizes, the $P6_1$ and $Fddd$ structures were treated separately and only the contributions of the dispersion folded to the Γ-point in super-cells containing 330 and 704 atoms, respectively, were considered; this is generally a good approximation due to the very large super-cells. The corresponding densities of states have been obtained by differentiating a spline interpolation of the integrated phonon density of states at the super-cell Γ-point. The integrated density $G(\omega)$ is given by

$$G(\omega) = \sum_{i=1}^{3N} \Theta(\omega - \omega_i), \tag{1}$$

with the Heaviside function $\Theta(\omega)$ and the phonon frequencies ω_i.

For perfect crystalline solids, the vibrational contribution to the free energy is most important, and can be calculated in the harmonic approximation from the normalized phonon density of states $g(\omega)$ as

$$F_{\text{vib}}(T) = r\,k_{\text{B}}T \int_0^\infty \mathrm{d}\omega\,g(\omega) \ln\left[2\sinh\left(\frac{\hbar\omega}{2k_{\text{B}}T}\right)\right], \tag{2}$$

where r is the number of degrees of freedom in the unit cell and k_{B} is Boltzmann's constant.

3. Analysis

The experimentally [6, 7, 9] and theoretically [4, 10, 11] proposed phases of Mg(BH$_4$)$_2$ vary significantly in density, coordination and complexity. In order to evaluate the stability of the proposed structures, we present the first comparison of the stability of the different Mg(BH$_4$)$_2$ phases based on DFT lattice free energy calculations. We have calculated the ground state energies and phonon density of states for the experimentally proposed $P6_1$ [6] and $Fddd$ [7] structures, and theoretically proposed $Pmc2_1$ [10], $P\bar{3}m1$ [4], and $I\bar{4}m2$ [11] phases. We furthermore present results for three other structures, a monoclinic Pm (figure 2; coordinates and

Table 1. Calculated lattice parameters and Wyckoff coordinates of $I4_1/amd$-Mg(BH$_4$)$_2$.

$I4_1/amd$	$a = 8.252$ Å $c = 10.474$ Å
Mg	(4*a*) (0, 0.75, 0.125)
	(4*b*) (0, 0.25, 0.375)
B	(16*h*) (0, 0.4846, 0.2305)
H	(16*h*) (0, 0.6135, 0.2880)
	(16*h*) (0, 0.4970, 0.1142)
	(32*i*) (0.8368, 0.3745, 0.4902)

Table 2. Calculated lattice parameters and Wyckoff coordinates of $F222$-Mg(BH$_4$)$_2$.

$F222$	$a = 9.928$ Å $b = 11.183$ Å $c = 11.891$ Å
Mg	(4*a*) (0, 0, 0); (4*c*) (1/4, 1/4, 1/4)
B	(16*k*) (0.09904, 0.1383, 0.1316)
H	(16*k*) (0.1314, 0.1030, 0.2252)
	(16*k*) (0.1651, 0.08003, 0.06345)
	(16*k*) (0.1223, 0.2438, 0.1127)
	(16*k*) (0.9769, 0.8735, 0.8747)

Figure 1. The (a) $P\bar{3}m1$ ($\rho = 1.04$ g cm^{-3}) and (b) $Pmc2_1$ ($\rho = 0.88$ g cm^{-3}) and the proposed (c) Pm ($\rho = 0.91$ g cm^{-3}) and (d) $I4_1/amd$ ($\rho = 1.01$ g cm^{-3}) structures of Mg(BH$_4$)$_2$. The blue spheres represent the Mg atoms and the yellow tetrahedra the BH$_4^-$ groups. Note the small difference between the $Pmc2_1$ and the $I4_1/amd$ phases.

unit cell parameters in the supplementary material available at stacks.iop.org/JPhysCM/21/012203) phase, a tetragonal $I4_1/amd$ (figure 3(b); coordinates and lattice constants in table 1), and the orthorhombic $F222$ structure (figure 4; coordinates and unit cell parameters in table 2), which all capture the ideal local coordination and display interesting characteristics.

3.1. Structural coordination

In order to understand why Mg(BH$_4$)$_2$, in contrast to most metal borohydrides, apparently forms large superstructures, and to understand the significance of the structural contributions to the total energy, we first analyze the coordination of the proposed structures.

Based on this analysis, we propose a $I4_1/amd$ (figure 3(b)) structure, which has the same topology as the experimental structures and the high-density phase observed in [9].

All the Mg(BH$_4$)$_2$ structures compared here show a tetrahedral arrangement of BH$_4^-$ ions around the Mg ion, except for $P\bar{3}m1$ proposed by Nakamori *et al* [4], which consists of identical layers of edge-sharing octahedra. For all the tetrahedral structures, the tetrahedra are corner sharing, but the connection of the coordination polyhedra is much more complex for the α- and β-phases than for the theoretically proposed phases [7].

The octahedral $P\bar{3}m1$ phase can be interpreted as consisting of an ABAB⋯ stacking of boron planes with magnesium in half of the octahedral interstices (figure 1(a)), and it is the most dense of the structures, with a density of 1.04 g cm^{-3}. This structure is in essence close packed, and therefore provides an upper bound of the mass density that can be achieved. The dense $Pmc2_1$, Pm, and $I4_1/amd$ structures follow an ABCABC⋯ stacking (figures 1(b)–(d)). The Pm phase is the smallest structure (11 atoms per unit cell) which captures the optimal primary coordination.

The new $I4_1/amd$ corresponds to two identical $I\bar{4}m2$ sub-lattices of corner-sharing tetrahedra folded into each other
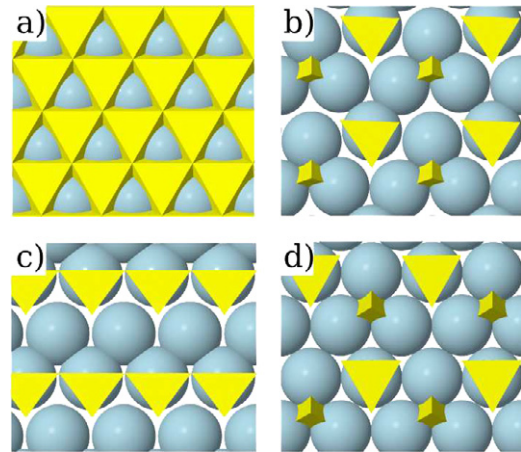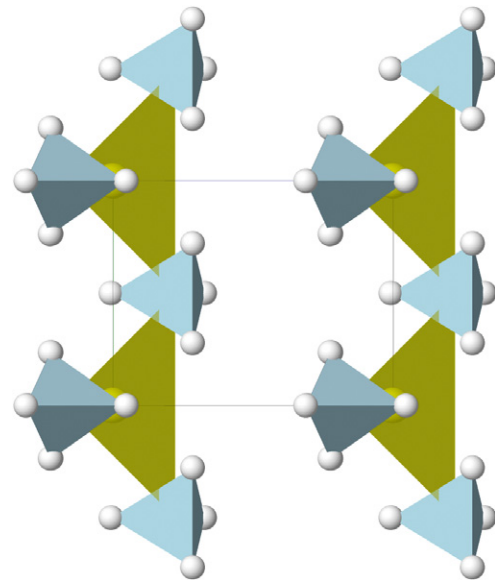

Figure 2. The structure of Pm. Yellow tetrahedra represent the Mg–B coordination and blue tetrahedra the BH$_4^-$ groups.

and thereby forming a close-packed structure (figure 3(b)). The main difference between the $I\bar{4}m2$, $I4_1/amd$, and $F222$ structures and the previously proposed theoretical ones lies in the arrangement of the polyhedra; the latter being layered and the first forming 3D networks, as observed for the experimental structures. Where the experimental structures have huge unit cells with five, eight, and ten membered rings of tetrahedra in $P6_1$ and four and eight membered rings in $Fddd$, the $I\bar{4}m2$ unit is much simpler and has only one kind of six membered rings. In $P6_1$ the rings penetrate each other, while for $I4_1/amd$ the rings belonging to each of the two $I\bar{4}m2$ sub-lattices penetrate the other (figure 5).

In the following, the influence of the differences in coordination on the structural stability is studied energetically,
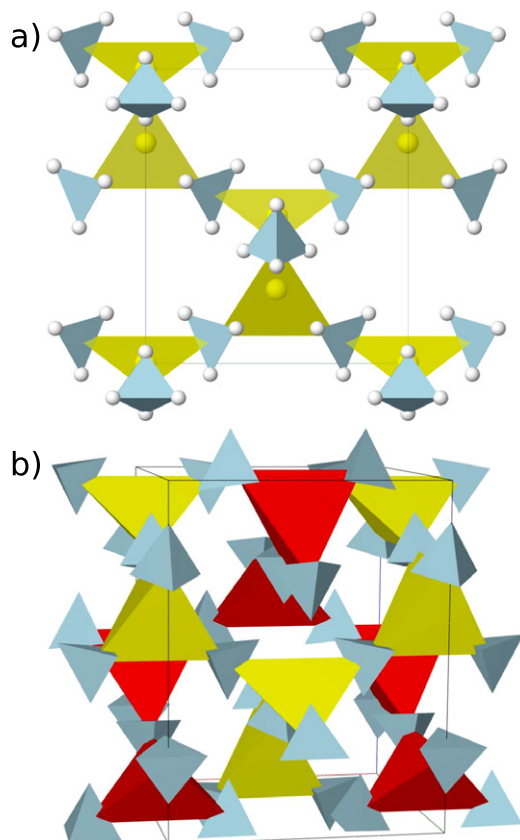
Figure 3. The (a) $I\bar{4}m2$ and (b) $I4_1/amd$ structures of $Mg(BH_4)_2$. Note the similarity of the $I4_1/amd$ phase to a double-folded $I\bar{4}m2$ structure. The yellow and red tetrahedra show the coordination of the B atoms around the Mg atoms. Blue tetrahedra represent the BH_4^- groups.

Table 3. Comparison of densities and ground state and lattice free energies per formula unit (ΔE_{gs} (relative to ground state energy of $P6_1$) and F_{vib}, respectively) of the considered $Mg(BH_4)_2$ phases.

	ρ (g cm^{-3})	ΔE_{gs} (eV)	F_{vib} (eV) (300 K)
$F222$	0.54	-0.10	2.02
$I\bar{4}m2$	0.56	-0.09	2.06
$I4_1/amd$	1.01	0.14	2.04
$P6_1$	0.82	0.00	2.12
$Fddd$	0.90	0.10	2.09
$Pmc2_1$	0.88	0.14	2.02
Pm	0.91	0.23	2.00
$P\bar{3}m1$	1.04	0.35	2.07

taking into account both the ground state energy of the electron–ion system and the lattice free energy.

3.2. Electronic density of states (DOS)

To study the influence of changing the coordination on the electronic structure, the electronic densities of states have been calculated.

A comparison of the electronic density of states (DOS) for the proposed structures (see figure 6) shows only small differences between the shapes of the DOS. All phases are insulators with calculated band gaps of around 6 eV.

The electrostatic ion–ion and ion–electron interaction energy is significantly higher for the low-density $I\bar{4}m2$ and
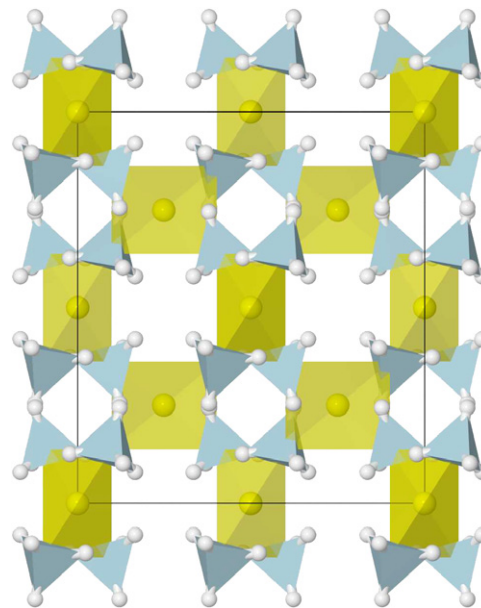

Figure 4. The structure of $Mg(BH_4)_2$ in space group $F222$ (blue tetrahedra, coordination of the B atoms; yellow tetrahedra, coordination of Mg with B atoms).
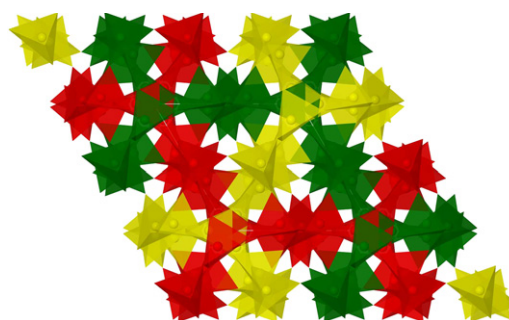

Figure 5. The structure of $P6_1$ $Mg(BH_4)_2$. Shown are the Mg–B tetrahedra. Different colors are used to distinguish different coordination rings.

$F222$ phases than for the other phases. This energy difference is slightly overcompensated by lower electronic energies, resulting in a lower total energy for the $F222$ phase (see table 3) than all other previously proposed structures (the electronic densities of states in figure 6 are plotted against the Fermi levels; the Fermi level is e.g. 1.54 eV lower per formula unit for the $F222$ than for, e.g., the $P6_1$ phase).

3.3. Phonon DOS

To investigate the stability and the influence of the structural differences on the vibrational free energies and the decomposition temperatures, we have calculated the phonon densities of states (PDOS) for the different phases.

Figure 7 shows the calculated PDOS for the analyzed structures. All spectra share general characteristics consisting of three separate bands (except for $P\bar{3}m1$, which shows further splitting). The low frequency regime at 0–20 THz is due to acoustic modes and optical modes in the magnesium/boron
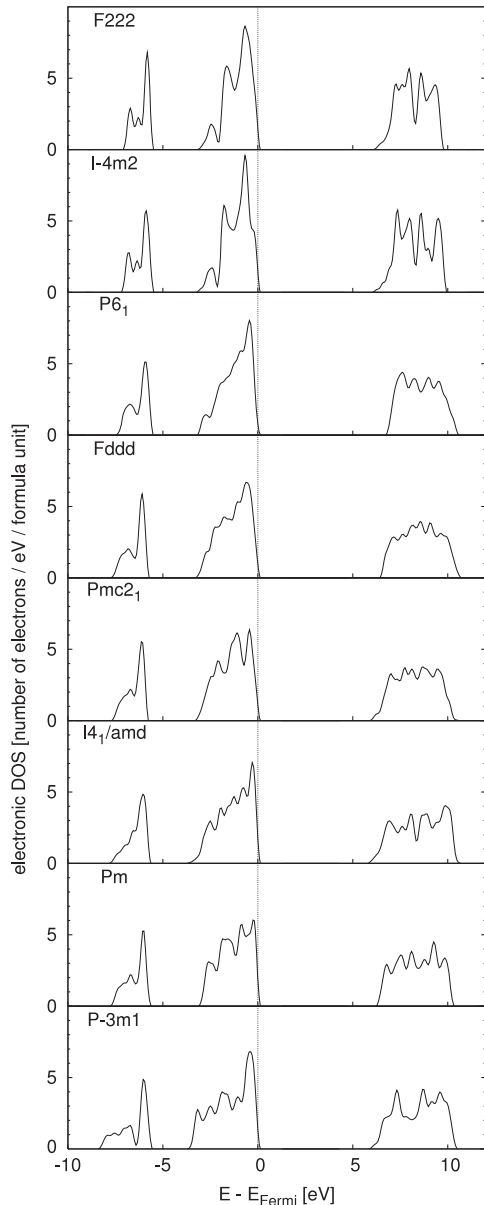
Figure 6. Electronic densities of states for different phases of $Mg(BH_4)_2$ plotted relative to the respective Fermi energies.

Figure 7. Normalized phonon densities of states for different phases of $Mg(BH_4)_2$. Imaginary frequencies are represented by negative real values. The dashed lines indicate the error of 0.1 THz^{-1} per mode in the PDOS associated with the modes, due to the numerically unresolved translational symmetry.

framework, the medium range (30–40 THz) corresponds to libration modes, and the narrow high frequency regime at $\sim$70 THz to B–H stretching vibrations.

The PDOSs of the structures are very similar, in particular for the most stable $F222$, $I\bar{4}m2$, $I4_1/amd$ and $P6_1$ phases (the $Pmc2_1$ phase was recently shown to be unstable by Ozolins *et al* [11]), all displaying optical modes in the low frequency domain and a very narrow B–H stretching band. In contrast to the other phases, the librational band of the $P\bar{3}m1$ phase is split into two peaks, caused by the differences in primary structure.

The existence of imaginary modes not resulting from numerically unresolved symmetries (see figure 7) is an indication of phase instabilities; the corresponding atomic displacements can, however, be followed in order to determine the stable phase. The uncertainty in PDOS per mode due to
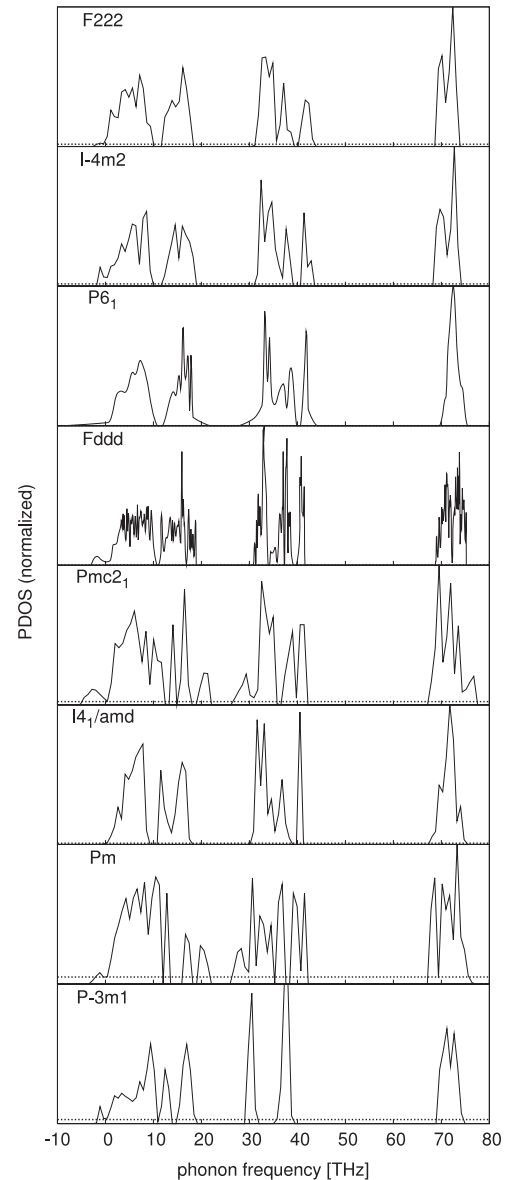
the numerically unresolved translational invariance is about 0.1 THz^{-1} in the systems considered, as indicated by dashed lines in figure 7.

We have analyzed the phonon dispersion of the most promising previously proposed $I\bar{4}m2$ structure in detail. At the Γ-point, all frequencies are real within the range of numerical accuracy. At the N-point of the Brillouin zone (the center of the zone facet) two acoustic modes become unstable. This is an indication of instability due to long wavelength acoustic vibrations. Instability of the low frequency acoustic phonons can be detected via macroscopic deformation of the unit cell. Indeed, an $\epsilon_{x,y}$ shear deformation combined with a relaxation of the internal degrees of freedom and the volume of the unit cell leads to a lowering of the total energy by 6 meV/f.u.

In order to identify the corresponding ground state structure, we have simultaneously imposed atomic coordinate displacements corresponding to the above mentioned unstable modes of the $I\bar{4}m2$ phase. Following the atomic displacements of these modes, we find that the conventional $I\bar{4}m2$ cell is distorted (in agreement with the shear instability mentioned above) to the primitive cell of a structure in space group $C222_1$ and further to $F222$ symmetry (containing 22 atoms per primitive cell). The ground state energy of the $F222$ phase is lower by 10 meV/f.u. compared to the $I\bar{4}m2$ phase. The phonon dispersion of the $F222$ phase shows, within the numerical accuracy, no imaginary frequencies, and we do not find any instabilities with respect to lattice strains, supporting the thermodynamic stability. Also for the proposed $I4_1/amd$ phase, the numerically calculated PDOS is free of imaginary modes, which supports a meta-stability and possible high-pressure existence of this high-density structure.

A zone boundary instability of acoustic modes in the $I\bar{4}m2$ structure points out that a normal mode analysis at the Γ-point may fail in predicting meta-stability of the structure. Therefore, calculations of the stability of the structure with respect to a macroscopic deformation of the unit cell should be applied as an additional measure. For stable structures, deformation of the unit cell leads to an increase in energy according to the elastic properties of the compound ($E_{tot} \sim C\epsilon^2$, where E_{tot} is the total energy of the system, C is the elastic constant, and ϵ is the deformation tensor of the unit cell). A deviation from harmonic behavior, especially a decrease of the total energy for strained structures, indicates a negative value of C, and therefore that the given structure is thermodynamically unstable with respect to macroscopic deformations.

3.4. Free energies

The free energies of the structures determine the relative stability of the different phases. In order to predict at which temperatures phase transitions would occur, we have calculated the lattice free energies from the PDOS above using equation (2). In order to show that the decomposition temperature of $Mg(BH_4)_2$ can be estimated, even if a stable ground state structure is not known, we have also calculated free energies in the presence of unstable modes by omitting the corresponding imaginary part (~1% integrated PDOS for the unstable structures) of the PDOS from the integration in equation (2).

Plotting the change in free energy as a function of temperature relative to the low-temperature $P6_1$ phase (figure 8), we find the free energy differences for the $Mg(BH_4)_2$ phases to be relatively small owing to the similar PDOSs. The calculated ground state energies (see table 3) are also quite similar, differing by less than 0.1 eV per H_2 (typically <0.05 eV), even though a comparison of the mass densities shows a large variation for the different phases. The simple tetragonal $I\bar{4}m2$ and orthorhombic $F222$ phases are unique, having the lowest ground state energies and a significantly lower density than the other phases. The stable $F222$ structure has the lowest energy of all investigated $Mg(BH_4)_2$ phases.

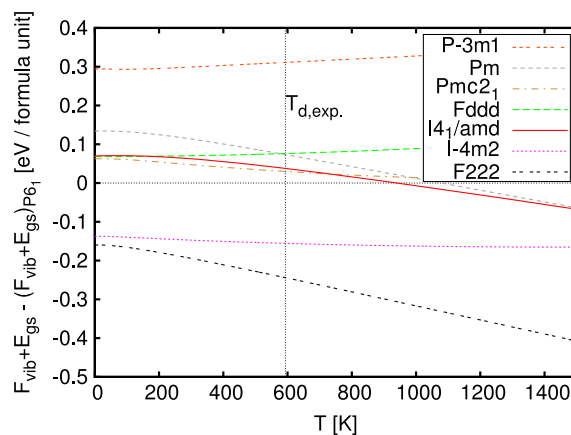**Figure 8.** Comparison of free energies with respect to the $P6_1$ low-temperature phase. $T_{d,exp.} = 320\,°C$ is the experimentally determined temperature for the first decomposition step of $Mg(BH_4)_2$ [8].

The phase with third lowest energy is the $P6_1$ phase. According to our calculations, none of the free energies of the higher energy phases cross that of the $P6_1$ phase below the experimentally determined initial decomposition temperature [8] of 320 °C (figure 8). The $P\bar{3}m1$ (erroneous coordination), and surprisingly also the $Fddd$ phase, show no intersection with the free energy of the $P6_1$ phase at all in the temperature range considered here. We note that the $Fddd$ phase is reported to be composed of disordered layers parallel to the b, c-plane [7], which gives rise to entropic contributions not considered here; both ground state configuration and free energy might therefore be different for the experimentally observed phase. Other non-phononic degrees of freedom, like rotations, will furthermore be of relevance at elevated temperatures [23].

To assess or predict at which temperatures the corresponding most stable phases would decompose to release hydrogen, the free energies of the decomposition products also have to be determined.

3.5. Desorption temperatures

The decomposition of $Mg(BH_4)_2$ was recently proposed to proceed in several steps including the formation of dodecaboranate species [8, 24], but to assess the stability of $Mg(BH_4)_2$ we consider only the following idealized decomposition step:

$$Mg(BH_4)_2 \rightarrow MgH_2 + 2B + 3H_2. \quad (3)$$
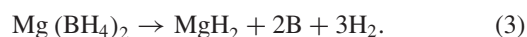
We estimate the desorption temperature by comparing the free energies of the $Mg(BH_4)_2$ phases to the Gibbs free energy of the right hand side of reaction (3) (we neglect pV terms for the solid phases). The lattice free energies of MgH_2 (space group $P4_2/mnm$) and B (space group $R\bar{3}m$) have been calculated using the software package Phonon [22], and values for the Gibbs free energy of H_2 have been interpolated from data in [25].

The temperature dependence of the free energies is shown in figure 9. The desorption temperature for reaction (3) can be
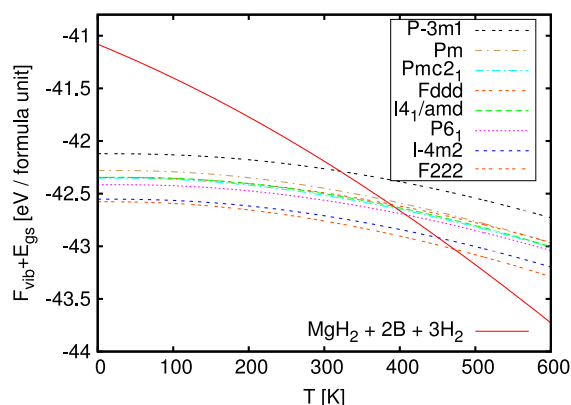
Figure 9. The sum of ground state energy E_{gs} and lattice free energy F_{vib} per formula unit for the different phases of $Mg(BH_4)_2$ and the decomposition products $MgH_2 + 2B + 3H_2$.

estimated to be 400–470 K for all phases with correct primary coordination. Especially if we disregard the high energy of the configurationally different $P\bar{3}m1$ structure, the estimated desorption temperatures differ only a little compared to the accuracy of the DFT-based estimate.

Due to similar PDOSs, the proposed structures would all start to decompose at 400–470 K. This is ∼150 K below the experimentally observed decomposition temperature [8]. This high decomposition temperature is thought to be due to kinetic barriers (in a more complex reaction than (3) [24]) rather than thermodynamic equilibrium properties [8], which have been considered in the calculations presented here.

4. Conclusions

We have analyzed the structural stability of different candidate structures for the promising hydrogen storage material $Mg(BH_4)_2$.

The electronic and phonon density of states are very similar for the investigated phases, resulting in only very small differences in free energies for phases which obey the primary coordination of Mg. By analysis of the instability of the previously proposed $I\bar{4}m2$ phase with respect to a macroscopic transformation of the unit cell characterized by acoustic mode zone boundary instabilities, we have obtained a new structure with $F222$ symmetry. This phase is free of instabilities and has a lower free energy than all other previously proposed structures.

Decomposition temperatures of 400–470 K have been obtained. Since the calculated free energies for the different phases of $Mg(BH_4)_2$ are quite similar from simple systems to very large unit cells, thermodynamic screening studies in, e.g., ternary and quaternary borohydride systems are possible by considering only simple model unit cells for an estimate of the structural stability of these compounds, as long as the expected primary coordination is obeyed.

This means that simple model structures can be used to investigate structural stability of complex structures, even if the crystal symmetries are not known *a priori*. In alloyed systems, e.g. mixed Mg and Ca borohydride, a simple structure should

thus allow for tetrahedral and octahedral coordination of Mg and Ca with B atoms, respectively.

We have shown that acoustic instability can be easily detected by macroscopic deformation of the unit cell, constituting a simple method to determine corresponding structural stabilities beyond a vibrational analysis.

Acknowledgments

References

[1] Ohba N, Miwa K, Aoki M, Noritake T, Towata S I, Nakamori Y, Orimo S I and Züttel A 2006 *Phys. Rev.* B **74** 075110
[2] Łodziana Z and Vegge T 2004 *Phys. Rev. Lett.* **93** 145501
[3] Sarner S F 1966 *Propellant Chemistry* 1st edn (New York: Reinhold)
[4] Nakamori Y, Miwa K, Ninomiya A, Li H, Ohba N, Towata S, Züttel A and Orimo S 2006 *Phys. Rev.* B **74** 045126
[5] Wiberg E and Bauer R 1950 *Z. Naturf.* b **5** 397
[6] Černý R, Filinchuk Y, Hagemann H and Yvon K 2007 *Angew. Chem.* **119** 5867
[7] Her J H, Stephens P W, Gao Y, Soloveichik G L, Rijssenbeek J, Andrus M and Zhao J C 2007 *Acta Crystallogr.* B **63** 561
[8] Chłopek K, Frommen C, Leon A, Zabara O and Fichtner M 2007 *J. Mater. Chem.* **17** 3496
[9] Konoplev V N and Bakulina V M 1971 *Bull. Acad. Sci. USSR Div. Chem. Sci.* **20** 136 (Engl. Transl.)
[10] Vajeeston P, Ravindran P, Kjekshus A and Fjellvåg H 2006 *Appl. Phys. Lett.* **89** 071906
[11] Ozolins V, Majzoub E H and Wolverton C 2008 *Phys. Rev. Lett.* **100** 135501
[12] Dai B, Sholl D S and Johnson J K 2008 *J. Phys. Chem.* C **112** 4391
[13] Setten M J v, Wijs G A d, Fichtner M and Brocks G 2008 *Chem. Mater.* **20** 4952
[14] Riktor M D, Sørby M H, Chłopek K, Fichtner M, Buchter F, Züttel A and Hauback B C 2007 *J. Mater. Chem.* **17** 4939
[15] Hohenberg P and Kohn W 1964 *Phys. Rev.* **136** B864
[16] Kresse G and Furthmüller J 1996 *Phys. Rev.* B **54** 11169
[17] Kohn W and Sham L J 1965 *Phys. Rev.* **140** A1133
[18] Perdew J P, Chevary J A, Vosko S H, Jackson K A, Pederson M R, Singh D J and Fiolhais C 1992 *Phys. Rev.* B **46** 6671
[19] Perdew J P, Chevary J A, Vosko S H, Jackson K A, Pederson M R, Singh D J and Fiolhais C 1993 *Phys. Rev.* B **48** 4978
[20] Blöchl P E 1994 *Phys. Rev.* B **50** 17953
[21] Kresse G and Joubert D 1999 *Phys. Rev.* B **59** 1758
[22] Parlinski K, Li Z-Q and Kawazoe Y 1997 *Phys. Rev. Lett.* **78** 4063
    Parlinski K 2005 *Software Phonon* Cracow
[23] Łodziana Z and Vegge T 2006 *Phys. Rev. Lett.* **97** 119602
[24] Hwang S J, Bowman R, Reiter J, Rijssenbeek J, Soloveichik G, Zhao J C, Kabbour H and Ahn C 2008 *J. Phys. Chem.* C **112** 3164
[25] Ke X and Tanaka I 2005 *Phys. Rev.* B **71** 024117